LUNAR MIGRATION OF ICE IN SEASONAL TRANSIENT SHADOW. Kristen M. Luchsinger[1] and Nancy J. Chanover[1], [1]Astronomy Department, New Mexico State University (kluchsin@nmsu.edu)

Introduction: The sources of water in the inner Solar System remains an outstanding question in the field of planetary science. One avenue of addressing this ongoing question is by examining a nearby natural laboratory – the surface of the Moon – and its interactions with its environment in orbit around the Earth. The interaction between the lunar surface and the solar wind results in the *in situ* formation of OH and H_2O molecules on the surface of the Moon [1, 2]. Three processes – impact delivery, volcanic outgassing, and solar wind – likely all contributed to water ice deposits within lunar polar cold traps [3], albeit at different times in lunar history. Solar wind ion implantation contributed less ice overall than either impact delivery or volcanic outgassing [4], but continues to deliver ice into the modern era, and is largely responsible for the current transient ice population.

The study of lunar water ice has historically focused on stable ice deposits at the lunar poles, due to the potential for these stable ice deposits to store information about the ice delivery history to the Earth-Moon system over geologic time scales [5]. However, absorption spectra of OH/H_2O by the Moon Mineralogy Mapper on the Chandrayaan-1 spacecraft and the Stratospheric Observatory for Infrared Astronomy detected a second population: dynamic, diurnally active, transient ice [6, 7]. The goal of this work is to characterize possible behaviors of migratory, transient water ice deposits within locations with dynamic illumination conditions.

Methods: In this work, we use the Lunar Migration of Ice in Seasonal Transient Shadow (LunarMISTS) model to explore the short term behavior of transient ice deposits over the course of a lunar year in nine prominent south pole craters. We selected Cabeus, Haworth, Shoemaker, Faustini, Amundsen, Hale Q, Schrödinger, Idel'son L, and Sverdrup craters. These craters represent a range of environments at the lunar poles: large craters containing with PSRs, SSRs, and non-shadowed regions; small, fully shadowed craters; small and large craters with no shadowing; and high latitude craters, ridges, and inter-crater plains. We therefore explore transient ice deposit behavior under a range of possible lunar conditions.

For the LunarMISTS model, we approximated the transient ice system in 1D columns at specific locations near the lunar poles with three processes: incoming ice, vertically migrating ice, and outgoing ice. We treat incoming ice as a constant, while the vertical migration and outgoing ice are both temperature dependent. The columns span 2 meters of lunar subsurface in order to capture behavior of ice within different stability regions, specifically, the uppermost 10 cm, the uppermost 0.5-1 meter, and 1-2 meters. These regions capture transient deposits, the uppermost layers of potentially stable ice deposits, and deeper, buried stable ice deposits. By modeling all three together, we can capture interactions or behavior differences between transient and stable populations. We use timesteps of just under five minutes, as calculated for polar temperatures using the metric in [8] for the minimum time step necessary to capture changes in regolith thermal conductivity as the temperature changes. We ran the model over two lunar years in order to capture the behavior of ice during all seasonal transitions.

LunarMISTS uses a horizon tracing method, which finds the terrain with the highest elevation angle from the point of view of a specific location on the lunar surface in every direction, and compares the generated horizon with the elevation angle of the Sun at that latitude as it changes over the course of the year. We calculate the flux delivered to the surface whenever the Sun rises above the generated horizon. Increased surface temperature from radiation delivered to the surface by the Sun propagates downward through the 1D column. The rate of propagation depends on the local thermophysical properties of the regolith, including the thermal conductivity and the density, which change with both depth and temperature.

While the surface temperature and vertical temperature profile are changing, an influx of ice is also delivered to the surface, and diffuses at a rate that is sensitive to the local temperature. Ice is allowed to escape at any time in the model, but with a residence time that depends on the local temperature, resulting in almost no ice loss during lunar night. The LunarMISTS model produces vertical ice profiles throughout the model run, as well as tracks the quantity of ice escaping over time, for an overall view of the behavior of the transient ice deposits throughout the lunar year. We ran the LunarMISTS model on the Discovery cluster in the New Mexico State University High Performance Computing Group [9].

We ran the LunarMISTS model using a grid across our selected craters with a mesh of roughly ten kilometers between each point. We characterized locations as one of four archetypes based on illumination conditions. The four archetypes are Permanently Shadowed Regions (PSRs), Seasonally Shadowed Regions (SSRs), Non-Shadowed Type A Regions (NSTAs), and Non-Shadowed Type B Regions (NSTBs). We defined PSRs as regions where the sun never rises above the local horizon. We defined SSRs as regions where the sun rises above the local horizon at least once but fails to rise above the local horizon for at least one sunrise. Non-shadowed regions are regions where the sun rises above the local horizon every lunar day.

Results: We see different ice behaviors in all four archetypes. We see stable ice with slow migration in PSRs. In SSRs, ice is stable and migrates at faster rates than those seen in PSRs during lunar winter, but is heated above stability and removed during lunar summer [10]. We divide non-shadowed regions into two subtypes: non-shadowed type A (NSTA) and non-shadowed type B (NSTB). We define NSTAs as regions where all ice is lost due to the sunrises, and NSTBs as regions where some ice is retained even after illumination and heating during the lunar winter. In Figure 1, we show four common behaviors seen in SSRs and NSTBs - the two archetypes that demonstrate dynamic transient ice behavior. Panel (a) shows an SSR in Cabeus crater with ice retention during the lunar winter and ice removal during the lunar summer, and a temporal lag due to the time needed for surface temperature increases to propagate downward into the column. Panel (b) shows a NSTB in Cabeus crater with SSR-like behavior. Ice is retained during winter months even when illuminated, indicating that the surface temperature increased, but did not maintain instability temperatures for longer than the residence time at that temperature. Panel (c) shows a NSTB in Amundsen crater with interrupted SSR-like behavior - that is, some ice is removed during lunar winter illumination, but it is an incomplete ice removal. Finally, panel (d) shows a NSTB in Haworth crater where surface ice is completely removed during the winter months, but some ice at depth is retained during the lunar winter day. Ice in all three non-shadowed regions is ultimately unstable, and does not result in the build up of stable ice deposits. Because we model over a short time frame, we do not include effects such as impact gardening that would significantly alter long-term stability, but that operate as stochastic events with an average event frequency far less than one event per year. Our results are therefore not applicable for studies of long term ice stability, but rather describe highly local potential behaviors of transient ice deposits over short time scales.

We found that all non-shadowed regions above 80° latitude are NSTBs, due to low sun angles during lunar winter. Our findings are consistent with the thermal pump effect described in [10], and suggest that this effect, extended into warmer areas where the thermal pump effect does not result in deeper stable or semi-stable deposits, still produces dynamic behavior. The results of this behavior are a temporal lag between surface illumination and ice removal, as well as lingering ice beneath the surface during lunar winter days in some locations.

Conclusions: The source of water delivery to the Earth-Moon system remains an unanswered question. Over geologic time scales, water ice that was formed on the surface of the Moon by interactions between solar wind protons and oxygen in lunar rocks is balanced by impact gardening, and is therefore unlikely to contribute significantly to ancient water ice deposits [4]. However, these transient ice deposits may exhibit short term dynamic behavior, particularly in SSRs or non-shadowed regions at very high latitudes. Dynamic behaviors include a temporal lag in escaping ice during lunar spring, semi-stable ice near the lunar surface during lunar winter, and incomplete removal of surface ice during short, cold lunar winter days. Observations of the temporal lag effect or semi-stable ice deposit depths could constrain migration rates of water ice at the lunar poles. Additionally, highly local incomplete removals of ice at the lunar surface could enable surface observations of ice during illuminated portions of the lunar day. Therefore, although transient ice deposits do not contribute to stable ice deposits over geologic time scales, they may exhibit dynamic short term behavior that could be leveraged to better constrain the behaviors of ice on the lunar surface.

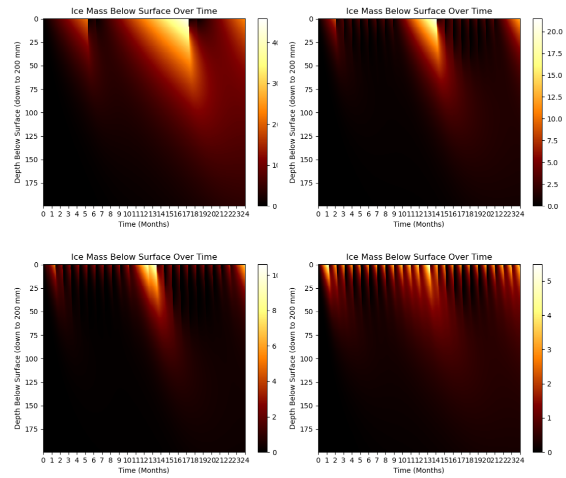

Figure 1: Heat map plots for four locations with color indicating the percent of ice retained, with the x axis representing time and the y axis representing depth. (a) Upper left, seasonally shadowed region. (b) Upper right, non-shadowed region type B with SSR-like behavior. (c) Lower left, non-shadowed region type B with interrupted SSR-like behavior. (d) Lower right, non-shadowed region type B with type A-like behavior.

References: **[1]** B. J. Butler. (1997) *JGR 102*, 19283–19292. **[2]** D. H. Crider et al. (2000) *JGR 105*, 26773–26782. **[3]** A. N. Deutsch et al. (2020) *336*, 113455. **[4]** P. G. Lucey et al. (2020) *LPSC LI*, 2319. **[5]** K. M. Cannon et al. (2020) *GRL 47*, e88920. **[6]** C. M. Pieters et al. (2009) *Science 326*, 568. **[7]** C. I. Honniball et al. (2020) *JGR (Planets) 125*, e06484. **[8]** P. O. Hayne et al. (2017) *JGR (Planets) 122*, 2371–2400. **[9]** S. Trecakov et al. (2021) *Assoc. for Computing Machinery 48*, 4. **[10]** N. Schorghofer et al. (2014) *APJ 788*, 169.